A Comparison Between Microstructure, Tensile Properties And Pitting Corrosion Resistance Of Friction Stir And Gas Tungsten Arc Ferritic Stainless Steel Welds

[1]G. Madhusudhan Reddy and [2]K. Srinivasa Rao
[1] Defence Metallurgical Research Laboratory, Hyderabad, 500 058, India
[2] Department of Metallurgical Engineering, A. U. College of Engineering (A), Visakhapatnam - 530 003, India.
*Corresponding author gmreddy_dmrl@yahoo.co.in

ABSTRACT

In the present work an attempt was made to study the pitting corrosion susceptibility of AISI 430 ferritic stainless steel welds. Gas tungsten arc (GTA) welding and friction stir welding (FSW) processes were used to make welds. Potentio-dynamic polarization test was used to evaluate pitting corrosion resistance of the welds. Optical and electron microprobe analysis were used to study the microstructure and corrosion mechanism respectively. It was observed that the weld microstructure of GTA weld was predominately columnar. Friction stir weld exhibited fine equiaxed grain structure. Investigations clearly revealed that pitting corrosion resistance of friction stir weld zone was inferior compared to GTA weld in which breakdown potential was reduced by chromium depletion. This was due to enhanced formation of intermetallic phase in friction stir welds compared to GTA welds. This was attributed to the slower cooling rate of friction stir welds, which results in longer exposure to the temperature range for precipitation during cooling cycle. Fine grain structure of friction stir weld has resulted in greater chromium depleted area than that of weld zone of GTA weld. In addition to the above, lower pitting corrosion resistance of friction stir welds was correlated to the formation of strain induced martensite in the nugget zone. Presence of residual stresses was also found to be affecting localized corrosion resistance by increasing number of active anode sites on the surface.

Key words: Piiting corrosion, Ferritic stainless steel, Welding, Microstructure, Sensitization.

1.0 INTRODUCTION

In the absence of nickel, the ferritic stainless steels are cheaper than austenitic grades and perform quite satisfactorily under milder service conditions. These steels are widely used in many industries such as automotive, chemical and architectural cladding because of their good mechanical properties and greater resistance to stress corrosion cracking. In addition to the above the notable feature of these alloys is that the scale formed on oxidation has nearly the same coefficient of thermal expansion as the matrix so that it remains protective in spite of cycles of heating and cooling which is not always the case with Cr-Ni or Cr-Ni-Mo alloys. However, when ferritic stainless steel is fusion welded chromium carbides were formed in the HAZ at locations exposed to temperatures above 900°C. This results in chromium depleted regions adjacent to the grain boundaries which deteriorates the corrosion resistance of the welded joint and the phenomenon is known as sensitization [1]. Because of the high chromium diffusion rate and low carbon solubility, sensitization develops rapidly in ferritic steels [2-4].

It can therefore be difficult or impossible to avoid sensitization completely by the use of low arc energy, especially if multipass welding is involved. In addition to the above, one of the major problems faced in fusion welding ferritic stainless steel is grain coarsening in weldments. These steels exhibit excess grain coarsening when material is exposed to temperature above 1150°C [5]. Refinement of grain size is not possible during post weld solidification due to absence of phase transformation

/allotropic modifications. Many methods for controlling the grain structure in weld metal have been reported in the literature and these include inoculation by the use of grain refining agents, vibration of the welding torch, current pulsation and magnetic arc oscillation [6]. Friction stir welding is a relatively new solid state joining process and has been the focus of constant attention in joining non weldable alloys [7]. FSW results in the formation of different microstructural regions like nugget or stirred zone, thermomechanically affected zone and heat affected zone. Dynamic recrystallization takes place in the nugget zone which leads to grain refinement. These characteristics of friction stir welds are likely to offer better properties than conventional fusion welds since FSW can avoid many problems associated with fusion welding processes such as solidification cracking, porosity and liquation cracking [8]. In a previous study [9], effect of microstructural evolution on corrosion properties of friction stir welded 304 stainless steel was studied. It was reported that small amount of sigma phases are rapidly formed along the grain boundaries in the advancing side of the stir zone having a dynamically recrystallized grain structure. Generally, sigma formation in austenitic stainless steels deteriorates the corrosion resistance [10]. In view of the above facts, a study has been taken up to develop an understanding on the corrosion behaviour of ferritic stainless steel welds. The study assumes special significance, as such studies are scarce. Present work is aimed at comparison of microstructure, tensile properties and pitting corrosion resistance of fusion zone of GTA weld and nugget zone of friction stir weld of AISI 430 ferritic stainless steel.

2.0 EXPERIMENTAL

The parent metal employed in this work is AISI 430 ferritic stainless steel. The chemical composition is given in **Table 1.** Steel plates in hot rolled and annealed condition each of size 300 mm x 80 mm x 3.2 mm were used for friction stir welding experiments. The plates were welded in single pass, normal to the rolling direction, with square-butt joint configuration employing a position controlled FSW machine (ETA make). The

Table 1 : Chemical composition of parent metals (Wt%)

Type of of Metal	C	Si	Mn	Cr	S	P	Fe
AISI 430	.06	.4	.4	17	.03	.04	Ba 1

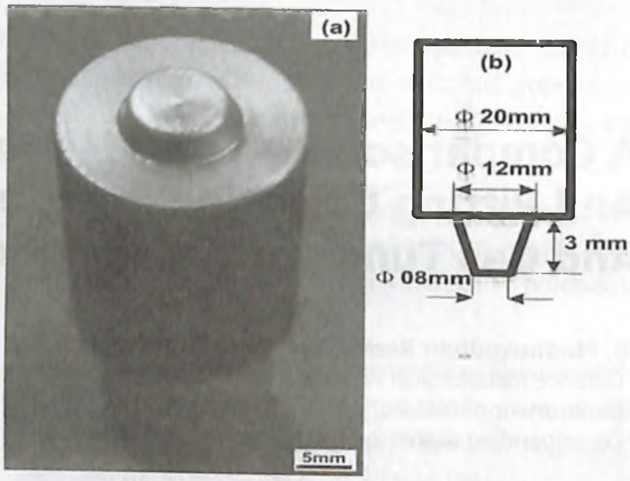

Fig.1: (a) W-Mo FSW tool (b) Schematic showing tool dimensions

initial joint configuration is obtained by securing the plates in position using mechanical clamps W-Mo tool is used in this investigation. Schematic of tool dimension and tool is shown in **Fig. 1**.

Experiments were carried out under a constant set of input process parameters, viz., spindle speed-800 rpm, travel speed-40 mm/min and tilt angle-2°. Direct current Gas tungsten arc welding (DC-GTAW) process with thoriated tungsten electrode of 2.4mm diameter and argon shielding gas with flow rate 20cmt/hr was employed to weld steel plates in square-butt joint configuration. GTA welding parameters of current 120A, voltage 20V and speed 120mm/min were used. Samples of the fusion zone of GTA weld and nugget zone of friction stir processed joint were sectioned and mounted in Bakelite. After mechanical polishing using 120 to 600 grit SiC papers the samples were polished using diamond paste on rotating wheels. Etching was done using aquaregia solution (3 parts HCl and part HNO3). Leitz optical microscope was used for recording the optical micrographs before and after corrosion. Longitudinal weld tensile test samples were machined as per the standard ASTM-E8. Tensile tests were conducted on Instron 1185 Universal testing machine at a cross head speed of 0.05mm/min. A software based GillAC basic electrochemical system was used to conduct potentiodynamic polarization tests to study the pitting corrosion behaviour of polished samples of fusion zone, nugget zone and the base metal. All experiments were conducted in an electrolyte of 0.5M H_2SO_4 + 0.5M NaCl. Steady state potential was recorded 10 minutes after immersion of the sample in to the electrode and the potential was raised anodically at a scan rate 2 mV/s. The potential at which the current increases abruptly after the passive region was taken as pitting potential (Epit). Specimens that exhibit higher positive potential value were considered to be those having better pitting resistance.

RESULTS AND DISCUSSION

Microstructure

Microstructure of the parent metal, ferritic stainless steel contains elongated grains of ferrite with dark precipitates at the grain boundaries are shown in the **Fig. 2.** Microstructural details across the cross section of the weld from centre to the interface of fusion zone of GTA weld central region consist of columnar grains, while in fusion boundary consists of equiaxed grains. This is due to characteristic feature of the gas tungsten arc welding thermal cycle which involves high temperatures and steep thermal gradients in relation to castings and the epitaxial nature of the growth process [11]. Microstructure of the friction stir weld across cross section is shown in **Fig. 4.** Friction stir weld region shows uniform and equiaxed grain structure covering entire weld region.

Formation of very fine and equiaxed grains of ferrite may be attributed to the dynamic recrystallization during friction stir welding.

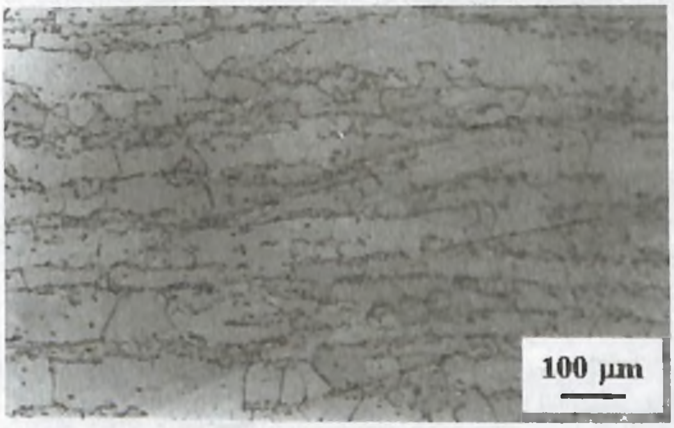

Fig. 2 : Microstructure of Base metal

Fig. 3 : Microstructure of GTA weld

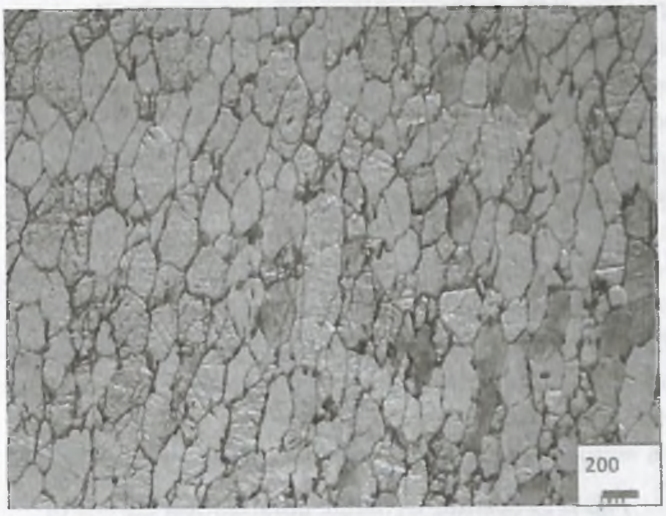

Fig. 4 : Microstructure of FS weld

Tensile properties

The results of tensile testing are shown in **Table 2.**

Table 2 : Tensile properties of welds

Type of weld	UTS (Mpa)	0.2% YS (MPa)	Elongation (%)
GTA Weld	430	325	3
FS Weld	750	435	28

As mentioned earlier, these were determined from longitudinal all-weld specimens taken from weld zone. The tensile data for each condition are an average of measurement made from three specimens. The superior strength and ductility of the longitudinal specimens of FS welds are commensurate with the observed grain refinement. The columnar grains, characteristic of GTA welds, were totally absent in FS welds (**Fig.4**). The higher ductility of FS welds could also be related to the fine and equiaxed grains.

Pitting corrosion

Typical polarization curves for parent metal, fusion zone of GTA weld and FS weld are shown in **Fig. 5**.

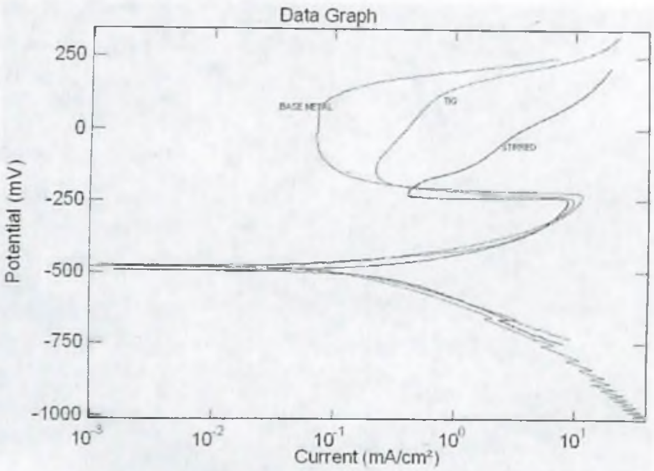

Fig. 5 : Potentio-dynamic polarization curves of GTA and FSWelds

Fig. 6 : Optical micrographs of GTA weld after corrosion

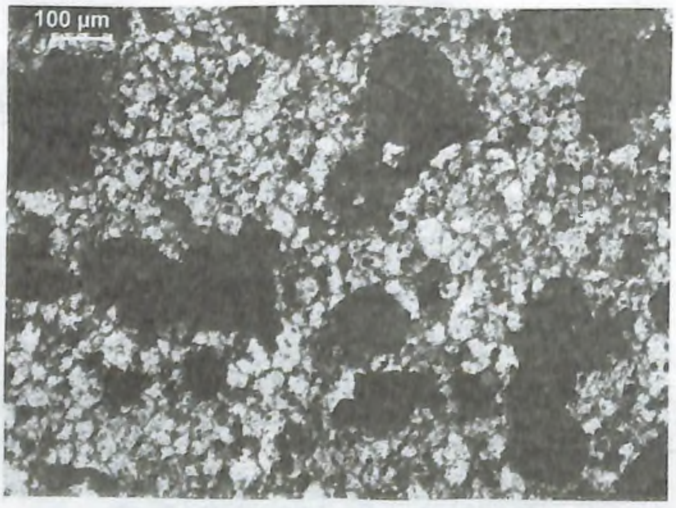

Fig. 7 : Optical micrograph of friction stir weld after corrosion

Pitting potential (E_{pit}) was taken as the criterion for comparison of pitting corrosion resistance. Less positive Epit values imply lower resistance to pitting, and vice versa. In general localized corrosion resistance of welds related to both precipitation effect and chemical segregation. Microstructural changes during friction stir welding may cause poor corrosion resistance in the stir zone when compared to parent metal and fusion zone of GTA weld. Optical micrographs GTA and FS welds after pitting corrosion tests are given in **Fig. 6** and **Fig.7** respectively.

It is very clear that all the grain boundaries of FS weld when compared to that of GTA weld zone under gone severe pitting which might have caused grain dropping. Chromium depleted zones are classically less corrosion resistant, thereby are attacked preferentially when the steel is exposed to corrosive environments.

The absence of chromium carbide precipitation in GTA welds might have resulted in higher pitting corrosion resistance compared to that of FS welds. This could be due to rapid solidification from the melt pool. This may lead to little time available for chromium enrichment at the dendritic interfaces. Poor corrosion resistance of friction stir welds could be due to the enhanced formation of intermetallic phase compared to GTA welds. This is attributed to the slower cooling rate of friction stir welds, which results in longer exposure to the temperature range for precipitation during cooling cycle. Carbon dissolves on heating ferritic stainless steel to temperature above 900°C and forms chromium carbide during cooling [12]. The reason for the enhanced precipitation of intermetallic phases in friction stir welds can not be exactly explained but it is likely attributable to high strain rates and recrystallization. It is likely that both introduction of high strain and dynamic recrystalization can accelerate mutual diffusion of the alloying elements, which possibly causes the rapid precipitation of intermetallic phases in the stir zone. Friction stir thermal cycle causes enhanced diffusion of chromium towards grain boundary. Observed chromium depletion may be contributed to the diffusion of chromium. Relatively higher magnitudes of plastic strains are induced in friction stir welds due to severe plastic deformation. These plastic strains may contribute to transformation induced martensite formation in the stir zone. XRD results (**Fig. 8**) clearly revealed the evidence of martensite in the stir zone. Similar phenomena was noticed in stainless steels by increasing cold working above 23% [13]

XRD results also confirm the duplex microstructure consisting of martensite in the ferritic matrix. Number of anodic sites

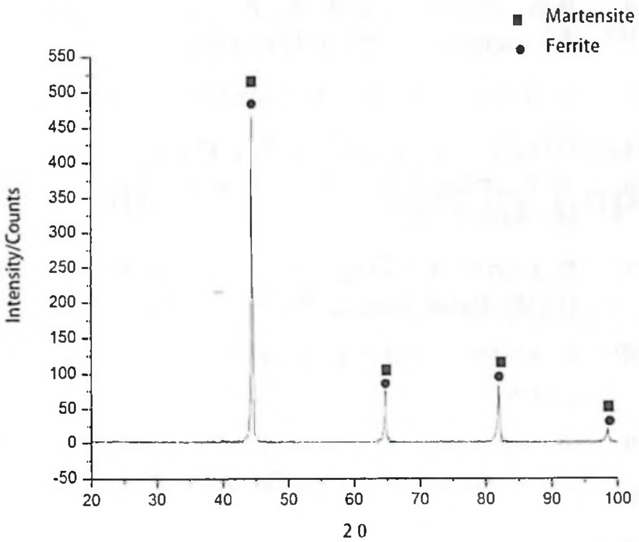

Fig.8 : XRD results of martensite in the stir zone of friction stir weld

belonging to martensite locations will increase and results in severe localized pitting corrosion. In addition to the above, the localized attack in stirred zone can also be explained as follows. Harmful anions, most notably the Cl- ion, have been shown to cause chemical breakdown of passive oxide films on stainless steels [14-17]. In stirred zone, internal stresses, often approaching the yield strength, may be produced [18]. Anions will migrate to stress gradients, which results in localized regions of high anion concentrations and in saline electrolytes, electrolysis reactions from corrosion can produce localized regions. Passivation breakdown in association with lack of spontaneous re-passivation in the presence of such electrolytes promotes accelerated localized attack [19]. This is in agreement with the present results on pitting corrosion of fusion zone and stirred zone of ferritic stainless steel. Observed phenomenon on the nugget zone is similar to sensitization or weld decay of heat affected zone of austenitic stainless steel fusion weld. In view of the above it is clearly understood that friction stir processing of ferritic stainless steel causes sensitization and poor corrosion resistance of nugget zone.

CONCLUSIONS

Microstructure of fusion zone of GTA weld of ferritic stainless steel was found to be columnar at the centre and to equiaxed at the fusion boundary which may be attributed to the thermal cycle during welding. Microstructure of the friction stir weld consisted of uniform and equiaxed grain structure covering entire weld region which may be attributed to the dynamic recrystallization during friction stir welding. The superior strength and ductility of the longitudinal specimens of FS welds when compared to GTA welds are commensurate with the observed grain refinement. The absence of chromium carbide precipitation in GTA welds might have resulted in higher pitting corrosion resistance compared to that of FS welds. Poor pitting corrosion resistance of friction stir welds of ferritic stainless steel was found to be due to chromium carbide depletion at the grain boundaries and transformation induced martensite. Hence the present investigation as established, friction stir welding may improve mechanical properties of ferritic stainless steel welds but adversely affects the pitting corrosion resistance of the welds when compared to gas tungsten arc welding.

ACKNOWLEDGEMENTS:

Authors would like to thank Director, Defence Metallurgical Research Laboratory (DMRL), Hyderabad for his constant encouragement and the permission to publish the work. Financial assistance from the Defence research and development organization (DRDO), New Delhi is gratefully acknowledged.

REFERENCES :

1. J. R. Davis (1994); Stainless steels, ASM Specialty hand book, ASM International.
2. E. Folkhard (1988); Welding Metallurgy of Stainless Steels , Vienna, Austria, Springer-Verlag.
3. J. E. Truman (1994); Stainless steels. Corrosion: Metal/Environment Reactions, 3rd edition. ed. by Shriver, L. L Jarman, R. A. and G. T Burstein, Oxford, U.K., Butterworth Heinemann, p. 334-377.
4. P. Bond (1969); Trans.Met.Soc of AIME 245(8), p.2127-2132.
5. S. Kou (1987); Welding metallurgy, John & Wiley publication, p.227 – 235.
6. D. W. Becker and C. M. Adams Jr. (1979); Welding J. 58 (5), p. 143-149.
7. W. H. Thomas, P. L. Threadgill and E. D. Nicholas (1999); Science and technology of welding and joining, 4, p.365-372.

8. R. S. Mishra and Z. Y. Ma (2005); Materials Science and Engineering, 50, p.1-11.

9. S. H. C. Park, S. S. Sutaka, K. Hiroyuki, O. Kazutaka and H. Satoshi (2004); Scripta Mate, 51, p.101-110.

10. K. N Krishnan, and K. Prasad Rao (1990); Werkstoffe and Korrosion 41, p.76-82.

11. J. C. Lippold and W. F. Savage (1979); Welding Journal, 58 (12), p.362-369.

12. C. John, Lippold and J. Kotecki (2005); Welding metallurgy and weldability of stainless steels, Wiley Interscience,

13. U. Kamachi Mudali, P. Shankar, S Ningshen, R. K Dayal, H. S Khatak and Baldev Raj (2002); Corr Science 44, p.2183-2190.

14. H.W Pickering, and R. P Frankenthal (1972); Electrochem Soc, 119, p.1297-1303.

15 N. D. Green and M. G Fontana (1958); Corrosion, 15, p.32-39.

16. W. E. White, J. Postlethwaite and I. Lemay (1976); Microstruct Sci, 9 p.1450-1457.

17. D. J. Chastell, P. Doig, P. E. J. Flewitt and P. J Norman (1988); Metall. Trans A, 19A, p.1445-1451.

18. R. A. Walker and T. G. Gooch (1991); Corrosion, 26, p.51-57.

19. R. Castrol and J. J Cadenet (1963); Welding metallurgy of stainless steels, London, Cambridge University Press.